Linked canyons and fans communicate through a migrating bedrock-alluvial transition

Li Zhang[1]*, Gary Parker[2]*, Jeffrey Nittrouer[3], Xudong Fu[4], Shanghong Zhang[1], Guangqian Wang[4]

*Corresponding authors: Li Zhang, Gary Parker, Email: 53802829@ncepu.edu.cn , parkerg@illinois.edu

ORCID: LZ: 0000-0002-9838-2718; GP: 0000-0001-5973-5296; JN: 0000-0002-4762-0157; XDF: 0000-0003-0744-0546; SHZ: 0000-0003-1131-2002; GQW: 0000-0002-5939-9138

[1*]School of Water Resources and Hydropower Engineering, North China Electric Power University, Beijing, China.

[2*]Department of Earth Science & Environmental Change and Department of Civil & Environmental Engineering, University of Illinois Urbana-Champaign, Urbana, IL, USA.

[3]Department of Geosciences, Texas Tech University, Lubbock, TX, USA.

[4]Department of Hydraulic Engineering, Tsinghua University, Beijing, China.

Abstract

The evolution of net-erosional fluvial landscapes is often treated separately from net-depositional fluvial landscapes, using different methods and different data input. Yet these landscapes are often tightly linked by means of a moving-boundary bedrock-alluvial transition. We consider a linked canyon-fan system in the setting of a Basin and Range province, basing our work loosely on Rainbow Canyon and Panamint Valley, Death Valley National Park, USA. The canyon is mixed bedrock-alluvial, and is incising into a plateau undergoing relative uplift. The fan is purely alluvial, and is part of a bajada complex in an adjacent valley undergoing relative subsidence. It might be thought that uplift would push the bedrock-alluvial transition out to the fault line denoting the canyon-fan boundary. Yet this transition is observed to be well up the canyon itself. Here we show that this behavior can be explained in terms of canyon-fan interaction captured by a single dimensionally homogeneous morphodynamic model which folds in both alluvial and incisional processes. We find that all other things being equal, increasing uplift rate tends to push the location of the transition valleyward, but under appropriate constraints the elevation of the transition point can be insensitive to uplift rate.

Steep, narrow canyons often link to wide alluvial fans[1]. The canyon is often bedrock-dominated, whereas the fan is alluvial. ("Bedrock" is shorthand for "mixed bedrock-alluvial"[2, 3].). We consider a linked canyon-fan system in a Basin and Range province such as the southwestern United States. Such provinces consist of subparallel mountain ranges undergoing relative uplift bounding valleys undergoing relative subsidence, corresponding to alternating horsts and grabens produced by deep-seated tectonic extension[4]. A series of canyons perpendicular to the range crest incise into the mountains, each emptying to fan. The fans often amalgamate to form a bajada[1]. Basin and Range topography is not unique to the southwestern United States; two other examples are in east Asia[5, 6].

We consider the morphodynamics of a single linked canyon-fan system, loosely based on Rainbow Canyon and its fan within the Panamint Valley bajada, Death Valley National Park, USA[7]. Fig. 1a shows the region that motivates our study, including the Argus Range and Panamint Valley. Fig. 1b shows the V-shaped Rainbow Canyon. Fig. 1c shows the canyon, fan, and present location of the bedrock-alluvial transition. Fig. 1d is a definition diagram for our simplified morphodynamic model, in which Santa Rosa Wash is the alluvial feeder channel from Darwin Plateau in the Argus range, B_c = width of the canyon channel (also taken to be the width of a virtual channel on the fan), B_d = width of the depositional zone, and L = initial length of the initial canyon-fan system, evenly split between canyon and fan. (The length of the canyon subreach can change as a plateau-canyon knickpoint migrates upstream.). Sediment is supplied from Darwin Plateau beyond the canyon head. The watershed extends upstream into the Argus Range[8]. The canyon head (knickpoint) is characterized by three incisional cyclic steps[9, 10, 11]. The canyon itself is V-shaped lacking tributaries (Fig. 1b).

Bedrock-alluvial transitions are commonly observed where mountains give way to plains. One example is the Fall Line, eastern United States, marking the boundary between the Appalachian Piedmont and the coastal plain[12, 13]. Bedrock-alluvial transitions can correspond to divides in plant species type[14]. Fig. 1c shows that in the case of Rainbow Canyon the bedrock-alluvial transition occurs not at the canyon mouth, where the normal fault bounds uplifting and subsiding zones, but approximately halfway up the canyon (verified by a helicopter survey by the authors on October 22, 2023 and a ground survey by the authors on January 18-19, 2024). This feature presents a conundrum: *why does the uplifting mountain range not push the bedrock-alluvial transition to the canyon mouth?*

Experiments and morphodynamic modeling are powerful tools to study canyon-fan evolution. Morphodynamic models can link hydraulics, sediment transport, alluviation and incision to describe system evolution. Features such as tectonics, base level change and abrasion can be included. Experimental and field results have been used to verify morphodynamic models of alluvial fans and fan-deltas[15, 16, 17, 18]. Cellular models have been used to study linked uplands (including canyons) and fans[19, 20, 21]. These models do not, however, focus on the dynamics of a bedrock-alluvial transition. Bedrock-alluvial transitions have been modeled experimentally[22, 23, 24, 25]. Numerical models can reproduce the dynamics of migrating bedrock-alluvial transitions observed at experimental and field scale[26, 27, 28, 29]. None of these models incorporates bedrock incision.

Bedrock incision has been modeled using the stream power model, where the incision rate is linked to channel slope and upstream drainage area[30, 31]. While useful for many purposes in original and extended form[32, 33], the original form does not incorporate sediment transport dynamics, and thus cannot be straightforwardly linked to a depositional zone. The first model of incisional bedrock channels that incorporates sediment transport dynamics appears to be the saltation-abrasion model[2, 3, 34, 35], according to which incision occurs only when the bedrock has a partial cover of alluvium[2, 36]. This model captures bedrock incision mediated by particles striking the bedrock surface. The saltation-abrasion model can be linked to the Exner equation of sediment conservation to describe spatiotemporal morphodynamic evolution, as in the case of a model of incisional morphodynamics of a simplified configuration based on Rainbow Canyon[8]. That model is not linked to a fan downstream.

Here we present a single morphodynamic model incorporating a) alluvial morphodynamics using a standard sediment transport equation and the Exner equation of sediment conservation, b) incisional morphodynamics including below-capacity sediment transport mediated by the fraction of bedrock surface area p covered by alluvium, c) simplified tectonics (uplift and incision without extension), d) upstream knickpoint migration at the channel head, e) sediment from sidewall erosion and f) a downstream boundary condition for either a closed or open basin. The bedrock-alluvial transition point is not assumed, but rather captured where the cover fraction changes from $p < 1$ to $p = 1$.

Configuration, morphodynamic model and input parameters

Our formulation for incision is the Macro-Roughness-based Saltation-Abrasion-Alluviation (MRSAA) model[37]. This model has been adapted for morphodynamic calculation based on the Moving-boundary Panamint Incision by Gravel Grinding (MOVING-PIGG) model[8]. Here we add a purely alluvial fan. The governing equations described in **Methods** constitute a unified model capturing canyon-fan morphodynamic interaction. Relevant caveats are listed there.

Our configuration is the simplified version of the Rainbow Canyon-Panamint fan system of Fig. 1d. It includes a) a tableland with slope S_p toward Panamint Valley (Darwin Plateau in the Argus Range) uplifting at constant rate υ, b) a non-incising feeder channel (Santa Rosa Wash) and an upstream-migrating canyon knickpoint, c) a V-shaped canyon with side slope S_s and initial length $L/2$, no tributaries and an incising canyon bottom with constant width B_c, d) a normal fault dividing the tableland and the valley (Fig. 1a), e) a valley basement subsiding at constant rate σ, f) an alluvial valley deposit (fan) of width B_d and constant length $L/2$, and g) a virtual channel on the deposit of the same width B_c as the canyon, but which implicitly spreads sediment deposits across the fan surface via migration-avulsion[15, 16]. Flood flows are intermittent, with constant flood discharge Q_w occurring at constant time fraction I_f. Where x is distance downstream of the initial position of the canyon head (which is a knickpoint initially at $x = 0$ km but which migrates upstream), the uplifting canyon extends to $x = L/2$, and the subsiding valley extends from $x = L/2$ to L. Canyon and valley slopes are S_c and S_v respectively; their initial values are S_{ci} and S_{vi}. Finally x_{ba} denotes the position of the bedrock-alluvial transition.

Other parameters include elevation of the bedrock surface η_b, thickness of the alluvial layer η_a above it, bed elevation $\eta = \eta_b + \eta_a$, areal fraction cover of alluvium over the bedrock surface p, bedrock incision rate E, grain size D of the gravel alluvium, submerged specific gravity R of the gravel particles, bed slope $S = - \partial\eta/\partial x$, dimensionless Chezy bed friction coefficient Cz, volume transport rate per unit width of sediment q_a, capacity sediment transport rate per unit width q_{ac}, upstream sediment feed rate q_{af}, bedrock abrasion coefficient β used in the relation for incision, fraction f_b of failed material from canyon sidewalls that remains as competent gravel on the canyon bottom and deposit porosity λ. Parameters that are common to all the runs here are given in Table 1, largely based on previous work[8]. Input parameters varied in the calculations are: σ, υ, B_d and f_b. We specify the ratio $r = B_d / B_c$ rather than B_d itself. The other parameters listed above are either specified or calculated based on the formulation in **Methods**. Downstream boundary conditions include a) free below-capacity outflow from basin[37] and b) closed basin.

Morphodynamics of pure incision and pure alluviation

Our goal is the morphodynamics of the bedrock-alluvial transition in a linked system of an uplifting canyon and subsiding fan. Before proceeding, we study model behavior under simpler conditions of pure incision and pure alluviation.

Results for pure incision are shown in Figs. 2a and 2b. In both cases the downstream "fan" (lower reach) is not actually a fan, but is instead a continuation of the canyon (upper reach) at half the slope S_b. The upper and lower reaches have the same width (r = 1). As outlined in **Methods**, the incision rate E in the upper reach is set at 3 mm/yr; a somewhat lower value prevails in the lower reach due to lower slope but invariant below-capacity sediment transport rate. The downstream boundary condition is free below-capacity sediment outflow. Sidewall erosion contributes no competent gravel to the bed, so $f_b = 0$.

In Fig. 2a uplift rate $\upsilon = 5$ mm/year. Uplift outpaces incision rate $E = 3$ mm/year everywhere, so bedrock elevation η_b increases over time, and the knickpoint migrates upstream at a slope that is higher than the upstream reach. In Fig. 2b uplift rate $\upsilon = 0.5$ mm/year; incision outpaces uplift, bedrock elevation everywhere decreases over time, and the knickpoint migrates upstream at a slope that is lower than the upstream reach. Under pure incision, bedrock slope remains temporally constant at its initial value. Were the uplift rate set equal to the incision rate of 3 mm/year and the lower reach have the same slope as the upper reach, nothing would change in time other than the upstream migration of the knickpoint. This is case is illustrated for the upper reach in Extended Fig. E1.

Results for pure alluviation are shown in Figs. 2c and 2d. Tectonics are turned off, so that $E = \upsilon = \sigma = 0$, and also $f_b = 0$. The bedrock basement remains fixed with the lower reach having half the slope of the upper reach, and r = 1. The downstream boundary condition is such that all sediment is captured (zero outflow; closed basin). Fig. 2c shows bedrock elevation η_b and elevation of the top of the alluvium η up to 1600 years. Alluvium is seen to passively onlap the bedrock basement. Fig. 2d shows a continuation of the calculation of Fig. 2c until alluvium spills onto the plateau.

Morphodynamics of the bedrock-alluvial transition as the canyon and fan interact with each other in a Basin and Range setting

We now capture canyon-fan interaction where the canyon uplifts and the valley subsides. As in Figs. 2a and 2b, upper-reach parameters are set so the bedrock incises at E = 3 mm/year wherever exposed. The fan (lower reach) subsides at $\sigma = 3$ mm/year in all cases, and r = 5, so the fan is 5 times wider than the canyon. The canyon (upper reach) uplifts at rates υ = 0, 3 and 5 mm/year. Sidewall failure does not produce competent gravel, i.e. $f_b = 0$.

Figs. 3a, 3b and 3c show bedrock elevation η_b and elevation η of top of the alluvium after 24,000 years for the cases $\upsilon = 0$, 3 and 5 mm/year. In Fig. 3d, the three results are superimposed.

These figures show three features capturing how the canyon and valley communicate with each other. a) For the case $\upsilon = 3$ mm/yr (Fig. 3a), onlapping of alluvium atop the bedrock turns off incision in the canyon, so that bedrock elevation rises downstream of the bedrock-alluvial transition. Uplift and incision balance upstream of this transition, so bed elevation does not change there. Onlapping onto the bedrock causes cessation of incision (blue box), reduces accommodation space (yellow box) and thus drives the bedrock-alluvial transition upstream faster than otherwise. b) A comparison of Figs. 3a and 3b shows that vanishing uplift does not give rise to concomitant loss in accommodation space, but a similar comparison of Figs. 3a and 3c shows that increased uplift exacerbates the loss in accommodation space. c) Fig. 3d shows that at 24,000 years, increasing uplift rate pushes the streamwise position x_{ba} of the bedrock-alluvial transition valleyward, indicating strong canyon-valley communication. The elevation η_{ba}, however remains invariant. This evidently implies a balance between the effect of net rise or fall of the bedrock reach upstream of the transition and net loss of accommodation space as alluviation turns off incision below the deposit. Although results are shown for only 24,000 years for clarity, they generalize for earlier and later times when a) the valley floor is no longer exposed and b) the alluvium has not yet spilled onto the plateau.

Fig. 4a shows a plot of η_{ba} and x_{ba} versus uplift, summarizing Fig. 3. Over the range $\upsilon = 0$ to 5 mm/year, the elevation of the transition remains constant. Increasing uplift rate pushes the position of the bedrock-alluvial transition valleyward, but not into the valley itself. This raises the question as to whether any rate of canyon uplift is sufficient to keep alluvium from onlapping the canyon floor. This issue is explored in Fig. 4b. All model conditions are the same as for Fig. 3a, except r is increased from 5 to 40, an 8-fold increase in the width of the accommodation space of the fan. The creation rate of accommodation space due to subsidence in the wide valley is so large that an uplift rate of 3 mm/year is sufficient to ensure that alluvium remains confined to the valley up to at least 19,200 years. Instead, a hanging valley, or waterfall appears at the canyon-fan transition[38]. This feature likely relaxes to sub-vertical and migrates upstream[11], but relevant mechanics are not included here. Such a waterfall, Darwin Falls, is seen two canyons south of Rainbow Canyon (inset of Fig. 4b). It is located about 5 km upstream of the mouth, and forms a waterfall due to a permanent spring. Raming and Whipple[39] have shown how such a feature can prevent the upstream transmission of base level fall, in this case induced by a high rate of production of accommodation space in the valley. Upstream of the waterfall in Fig. 4b, incision and uplift continue to balance. This example demonstrates how canyon and fan can fail to communicate with each other.

Several variant cases are shown in the Extended Figures. Extended Fig. E1 corresponds to Fig. 2 but considers pure incision with E balancing $\upsilon = 3$ mm/year in the upper reach. Nothing happens in that reach except upstream migration of the knickpoint. Extended Fig. E2 corresponds to Fig. 3a, but with punctuated uplift every 240 years rather than continuous uplift. Little difference is seen at sufficiently large time and space scales. Extended Fig. E3 corresponds to Fig. 3, but with a sediment sidewall input factor $f_b = 0.25$; it is seen that η_{ba} is no longer invariant to uplift rate. Extended Fig. E4 corresponds to Fig. 4a, but with a sediment sidewall input factor $f_b = 0.25$. Extended Fig. E5 shows the effect of heavy sidewall sediment input for 6000 years, and a reduction of the sediment feed rate to 1/100 beyond that time. The figure illustrates the ability of the model to capture multiple interacting drivers.

Discussion

We bring together in a simplified way tectonics, sediment transport, alluviation, incision and bed morphodynamics to link erosional and depositional processes in a canyon-fan system. This linkage advances the study of geomorphology at source-to-sink scale.

Our model is "1.5 D" (1D with extension to canyon sidewall erosion and channel migration on the fan). In this sense, it is less complex than 2D cellular models[19, 20, 21]. It does, however, include relations for sediment transport, cover and incision that have a strong basis in experimental and field research. It allows specific insight into canyon-fan interaction and migration of a bedrock-alluvial transition. Three novel results follow.

1. Canyon and fan can communicate with each other, in the sense that even when the canyon undergoes uplift, alluviation from downstream can push the bedrock-alluvial transition well into the canyon itself. This alluviation "turns off" incision by burying the bed, so that uplift there reduces the accommodation space for alluvium and pushes the transition even faster up the canyon (Fig. 3a).

2. When competent sediment delivered from canyon sidewalls is excluded, a set of conditions exist whereby at any given time (within some range) the streamwise position of the bedrock-alluvial transition in the canyon displaces downstream with increasing uplift rate, but the elevation of that point remains invariant (Figs. 3d and 4a).

3. When the valley is sufficiently wide compared with the canyon, however, alluvium may never onlap the canyon bedrock, and instead a hanging valley, or vertical face forms at the canyon mouth (Fig. 4b).

The effect of climate change could be included in part by changing the flood discharge and intermittency. Based on the results for punctuated uplift in Fig. E2, the model would not likely show a clear signal for cyclic climate change over hundreds of years. Changes in flood discharge and intermittency corresponding to inferred records of climate change over a glacial cycle would give rise to a signal. Death Valley itself is often partially or fully occupied by Lake Manly, especially during glacial periods. Lake Manly had highstands approximately 26,000, 18,000 and 12,000 years before present[40], and Panamint Valley was similarly occupied by Panamint Lake[41]. Under such circumstances, the model used to model the bajada (line fan) can be altered in a straightforward way to describe a line fan-delta[42] that responds to rise and fall of the lake level[43].

Methods

The methods used here largely follow previous work where more detailed information can be found[8]. We assume a single, non-abrading grain size of sediment with size D moving as bedload. During a flood, the flow is assumed to obey the normal assumption for momentum balance and a water conservation equation for constant width B_c. This allows the following relation between the Shields number of sediment mobility τ^* and channel slope S.

$$\tau^* = \left(\frac{Q_w^2}{Cz^2 g B_c^2} \right)^{1/3} \frac{S^{2/3}}{RD} \tag{1}$$

where Q_w is the flood water discharge, Cz is the dimensionless Chezy coefficient of bed resistance, g is the gravitational acceleration and R is the submerged specific gravity of the sediment (= 1.65 here). We calculate the sediment transport rate as follows:

$$q_a = p q_{ac} \tag{2a}$$

$$q_{ac} = 4\sqrt{RgD}\, D\left(\tau^* - 0.0495\right)^{3/2} \tag{2b}$$

where q_a is the volume rate of sediment transport rate per unit width, q_{ac} is the capacity transport rate[44] and p is an adjusted areal fraction of alluvial cover over the bed[2, 3, 8, 36, 45]. We parameterize p as follows:

$$p = \begin{cases} p_l + (p_h - p_l)\dfrac{\eta_a}{L_{mr}}, & 0 \le \dfrac{\eta_a}{L_{mr}} \le \dfrac{1-p_l}{p_h - p_l} \\ 1, & \dfrac{\eta_a}{L_{mr}} > \dfrac{1-p_l}{p_h - p_l} \end{cases} \tag{3}$$

where η_a is the thickness of the alluvial layer over bedrock or basement, L_{mr} is a macro-roughness characterizing the rugosity of the bedrock surface, $p_l = 0.05$ and $p_h = 0.95$. Here the value $L_{mr} = 1$ m[8]. The use of cover fraction p is equivalent to a mushy layer formulation[46].

Bedrock balance is treated as follows. In the canyon, where η_b = top of the bedrock surface and E is the bedrock erosion (incision) rate,

$$\frac{\partial \eta_b}{\partial t} = \upsilon - E \tag{4a}$$

$$E = I_f \beta q_a (1-p) \tag{4b}$$

where β is a coefficient of bedrock abrasion, here approximated as a prescribed constant. In the valley, the bed is assumed to be alluviated, so that the corresponding form of Eq. 4a for the valley basement is

$$\frac{\partial \eta_b}{\partial t} = -\sigma \tag{5}$$

The Exner equation of sediment conservation takes the following form in the canyon[8]:

$$(1-\lambda) B_c p \frac{\partial \eta_a}{\partial t} = -I\frac{\partial}{\partial x}(B_c q_a) + 2 f_b \frac{\eta_T - \eta_b}{S_s} I \beta q_a (1-p) \tag{6}$$

where λ is the porosity of the alluvial deposit. The last term on the right denotes the production of sediment from the sidewalls as the bed incises downward. Here η_T denotes the local top of the uplifting plateau, which is assumed to have slope S_p, and f_b denotes the fraction of failing sidewall material that is retained as competent bed material (rather than shattering to wash load). Wherever the canyon flow is completely alluviated ($p = 1$), the last term on the right of Eq. 6 is taken to be vanishing. The corresponding Exner equation for the valley is

$$(1-\lambda) B_c p \frac{\partial \eta_a}{\partial t} = -\frac{I}{r}\frac{\partial}{\partial x}(B_c q_a) \tag{7}$$

where $r = B_d / B_c$ is the ratio of the depositional width of the valley fan B_d to virtual channel width B_c, which for simplicity is assumed to equal the width of the channel at the bottom of the canyon. Elevation to the top of the bed η is given as

$$\eta = \eta_b + \eta_a \tag{8}$$

The equations are solved numerically using an upstream boundary condition of specified alluvial feed rate q_{af}. The downstream boundary condition can be either open (all sediment flows out[8, 37] or closed, in which case

$$q_a\Big|_{x=L} = 0 \tag{9}$$

The calculations use either a fixed spatial domain extending from $x = 0$ to $x = L$, or a moving boundary formulation which can track an upstream-migrating knickpoint at the canyon head[8].

We enumerate several caveats regarding the formulation. We assume constant canyon bottom width, whereas Rainbow Canyon is observed to widen downstream. We do not include basin extension[4]. We assume that deposition is driven by channelized fluvial processes, and do not include the effect of sheet or debris flows[1]. We assume a single bedrock lithology, whereas a complex pattern of lithology can be found in the area[47]. We assume a single sediment grain size D in transport that does not abrade, as opposed to multiple grain sizes that abrade[48]. We assume a constant hydrologic regime over 10's of thousands of years, whereas climactic oscillations have been inferred over at least the last 155,000 years[49, 50]. The uplift and subsidence rates used here are on the high side in order to illustrate morphodyamics over 10's of thousands of years, but are still of the correct order of magnitude[8, 51]. The flow model used here is a normal flow model and so cannot specifically capture the details of the morphodynamics of the three steps at the head of Rainbow Canyon. The flow model would have to be extended to a gradually varied backwater model to do this[52]. These myriad features are not included because a) the necessary parameters are highly site-specific and often difficult to constrain, and/or b) because their inclusion would obscure the several fundamental canyon-fan interaction processes elucidated herein. Complexities can be added as the need arises, with a corresponding change in the interpretation of model results.

Data availability

All data used herein are included in the text.

References

1. Blair, T. C. & McPherson, J. G. Chapter 14: Processes and Forms of Alluvial Fans. In "Geomorphology of Desert Environments". *Springer Dordrecht*, 413-467 (2009).
2. Sklar, L. S. & Dietrich, W. E. A mechanistic model for river incision into bedrock by saltating bed load. *Water Resour. Res.* **40**(6), W06301 (2004).
3. Sklar, L. S. & Dietrich, W. E. The role of sediment in controlling steady-state bedrock channel slope: Implications of the saltation-abrasion incision model. *Geomorphology* **82**(1-2), 58-83 (2006).

4. Stewart, J. H. Basin and range structure: A system of horsts and grabens produced by deep-seated extension. *Geol. Soc. Am. Bull.* **82**(4), 1019-1044 (1971).

5. Windley, B. F. & Allen, M. B. Mongolian plateau: Evidence for a late Cenozoic mantle plume under central Asia. *Geology* **21**(4), 295-298 (1993).

6. Zhou, J. P. et al. Differential uplift triggered basin-and-range system: Evidence from low-temperature thermochronology in Eastern NE Asia. *Tectonics* **43**(1), e2023TC007857 (2023).

7. Waskiewicz, T., Mihir, M. & Whitworth, J. Surface variability of alluvial fans generated by disparate processes, eastern Death Valley, CA. *Prof. Geogr.* **60**(2), 207-223 (2008).

8. Zhang, L., Li, T. J., Wang, G. Q., Nittrouer, J. A. & Parker, G. How canyons evolve by incision into bedrock: Rainbow Canyon, Death Valley National Park, USA. *Proc. Natl. Acad. Sci. U.S.A.* **117**(26), 14730-14737 (2020).

9. Scheingross, J. S. & Lamb, M. P. A mechanistic model of knickpoint plunge pool erosion into bedrock. *J. Geophys. Res. Earth Surf.* **122**, 2079-2104 (2017).

10. Scheingross, J. S., Lamb, M. P. & Fuller, B. M. Self formed bedrock knickpoints. *Nature* **567**, 229-233 (2019).

11. Scheingross, J. S., Limaye, A. B., McCoy, S. W. & Whittaker, A. C. The shaping of erosional landscapes by internal dynamics. *Nat. Rev. Earth Environ.* **1**(12), 661-676 (2020).

12. Pavich, M. J. Regolith residence time and the concept of surface age of the piedmont "Peneplain". *Geomorphology* **2**(1-3), 181-196 (1989).

13. Hupp, C. R. Hydrology, geomorphology and vegetation of Coastal Plain rivers in the south-eastern USA. *Hydrol. Process.* **14**, 2991-3010 (2000).

14. Nucci, A., Angiolini, C., Landi, M. & Bacchetta, G. Influence of bedrock-alluvial transition on plant species distribution along a Mediterranean river corridor. *Plant Biosyst.* **146**(3), 564-575 (2012).

15. Parker, G., Paola, C., Whipple, K. & Mohrig, D. Alluvial fans formed by channelized fluvial and sheet flow: Theory. *J. Hydraul. Eng.* **124**(10), 1-11 (1998a).

16. Parker, G. et al. Alluvial fans formed by channelized fluvial and sheet flow: Application. *J. Hydraul. Eng.* **124**(10), 12-20 (1998b).

17. Whipple, K. X., Parker, G., Paola, C. & Mohrig, D. Channel Dynamics, Sediment Transport, and the Slope of Alluvial Fans: Experimental Study. *J. Geol.* **106**, 677-693 (1998).

18. Sun, T., Paola, C., Parker, G. & Meakin, P. Fluvial fan-deltas: Linking channel processes with large-scale morphodynamics. *Water Resour. Res.* **38**(2), (2002).

19. Densmore, A. L., Allen, P. A. & Simpson, G. Development and response of a coupled catchment fan system under changing tectonic and climatic forcing. *J. Geophys. Res.* **112**, F01002 (2007).

20. Pepin, E., Carretier, S. & Herail, G. Erosion dynamics modelling in a coupled catchment-fan system with constant external forcing. *Geomorphology* **122**, 78-90 (2010).

21. Welivitiya, W. D. D. P., Willgoose, G. R. & Hancock, G. R. Geomorphological evolution and sediment stratigraphy of numerically simulated alluvial fans. *Earth Surf. Process. Landf.* **45**, 2148-2166 (2020).

22. Muto, T. Shoreline autoretreat substantiated in flume experiment. *J. Sediment. Res.* **71**, 246-254 (2001).

23. Muto T. & Steel, R. J. Autostepping during the transgressive growth of deltas: Results from a flume experiment. *Geology* **29**, 771-774 (2001).

24. Kim, W. & Muto, T. Autogenic response of alluvial-bedrock transition to base-level variation: Experiment and theory. *J. Geophys. Res. Earth Surf.* **112**(F3), (2007).

25. Kim, Y., Kim, W., Cheong, D., Muto, T. & Pyles, D. R. Piping coarse-grained sediment to a deep water fan through a shelf-edge delta bypass channel: Tank experiments. *J. Geophys. Res.* **118**(4), 2279-2291 (2013).

26. Parker, G., Muto, T., Akamatsu, Y., Dietrich, W. E. & Lauer, J. W. Unraveling the conundrum of river response to rising sea level: from laboratory to field. Part I. Laboratory experiments. *Sedimentology* **55**(6), 1643-1655 (2008a).

27. Parker, G., Muto, T., Akamatsu, Y., Dietrich, W. E. & Lauer, J. W. Unraveling the conundrum of river response to rising sea level: from laboratory to field. Part II. The Fly-Strickland River System, Papua New Guinea. *Sedimentology* **55**(6), 1657-1688 (2008b).

28. Viparelli, E., Nittrouer, J. A. & Parker, G. Modeling flow and sediment transport dynamics in the lowermost Mississippi River, Louisiana, USA, with an upstream alluvial-bedrock transition and a downstream bedrock-alluvial transition: Implications for land building using engineered diversions. *J. Geophys. Res.* **120**(3), 534-563 (2015).

29. Jafarinik, S. & Viparelli, E. Alluvial morphodynamics of low-slope bedrock reaches transporting nonuniform bed material. *Water Resour. Res.* **56**, e2020WR027345 (2020).

30. Howard, A. D. A detachment-limited model of drainage basin evolution. *Water Resour. Res.* **30**, 2261-2285 (1994).

31. Whipple, K. X. & Tucker, G. E. Dynamics of the stream-power river incision model: Implications for height limits of mountain ranges, landscape response timescales, and research needs. *J. Geophys. Res. Solid Earth* **104**(B8), 17661-17674 (1999).

32. Gasparini, N. M. & Brandon, M. T. A generalized power law approximation for fluvial incision of bedrock channels. *J. Geophys. Res. Earth Surf.* **116**(F2), (2011).

33. Lague, D. The stream power river incision model: Evidence, theory and beyond. *Earth Surf. Process. Landf.* **39**, 38-61 (2014).

34. Chatanantavet, P. & Parker, G. Experimental study of bedrock channel alluviation under varied sediment supply and hydraulic conditions. *Water Resour. Res.* **44**(12), (2008).

35. Chatanantavet, P. & Parker, G. Physically based modeling of bedrock incision by abrasion, plucking, and macroabrasion. *J. Geophys. Res.* **114**, F04018 (2009).

36. Turowski, J. M., D. Lague D. & Hovius, N. Cover effect in bedrock abrasion: A new derivation and its implications for the modeling of bedrock channel morphology. *J. Geophys. Res. Earth Surf.* **112**(F4), (2007).

37. Zhang, L., Stark, C. P., Schumer, S., Fu, X. D., Kwang, J., Li, T. J. & Parker, G. The advective-diffusive morphodynamics of mixed bedrock-alluvial rivers subjected to spatiotemporally varying sediment supply. *J. Geophys. Res. Earth Surf.* **123**(8), 1731-1755 (2018).

38. Crosby, B. T., Whipple, K. X., Gasparini, N. M. & Wobus, C. W. Formation of fluvial hanging valleys: Theory and simulation. *J. Geophys. Res. Earth Surf.* **12**(F3), (2007).

39. Raming, L. W. & Whipple, K. X. When knickzones limit upstream transmission of base-level fall: An example from Kaua'i, Hawai'i. *Geology* **50**, 382-1386 (2022).

40. Hershler, R., Mulvey, M. & Liu, H. P. Biogeography in the Death Valley region: Evidence from springsnails (Hydrobiidae: Tryonia). *Zool. J. Linn. Soc.* **126**(3), 335-354 (1999).

41. Jayko, A. S., et al. Late Pleistocene lakes and wetlands, Panamint Valley, Inyo County, California. In "Late Cenozoic Drainage History of the Southwestern Great Basin and Lower Colorado River Region: Geologic and Biotic Perspectives". *Geological Society of America Special Paper* **439**, 151-184 (2008).

42. Kostic, S. & Parker, G. Progradational sand-mud deltas in lakes and reservoirs. Part 1. Theory and numerical modeling. *J. Hydraul. Res.* **41**(2), 127-140 (2003).

43. Parker, G., Muto, T., Akamatsu, Y., Dietrich, W. E. & Lauer, J. W. Unraveling the conundrum of river response to rising sea level: from laboratory to field. Part II. The Fly-Strickland River System, Papua New Guinea. *Sedimentology* **55**(6), 1657-1688 (2008).

44. Wong, M. & Parker, G. Reanalysis and correction of bed-load relation of Meyer-Peterand Müller using their own database. *J. Hydraul. Eng.* **132**(11), 1159-1168 (2006).

45. Zhang, L. et al., Macro-roughness model of bedrock-alluvial river morphodynamics. *Earth Surf. Dyn.* **3**, 113-138 (2015).

46. Voller, V. R. & Prakash, C. A fixed grid numerical modelling methodology for convection-diffusion mushy region phase-change problems. *Int. J. Heat Mass Transf.* **30**(8), 1709-1719 (1987).

47. Geist, E. L. & Brocher, T. M. Geometry and subsurface lithology of southern Death Valley basin, California, based on refraction analysis of multichannel seismic data. *Geology* **15**(12), 1159-1162 (1987).

48. Parker, G. Selective sorting and abrasion of river gravel: Applications. *J. Hydraul. Eng.* **117**(2), 150-171 (1991).

49. Woodcock, D. The late Pleistocene of Death Valley: A climatic reconstruction based on macrofossil data. *Palaeogeogr. Palaeoclimatol. Palaeoecol.* **57**(2-4), 273-283 (1986).

50. Menking, K. M., Bischoff, J. L., Fitzpatrick, J. A., Burdette, J. L. & Rye, R. O. Climatic/hydrologic oscillations since 155,000 yr B.P. at Owens Lake, California, reflected in abundance and stable isotope composition of sediment carbonate. *Quat. Res.* **48**, 58-68 (1997).

51. Labotka, T. C. & Albee, A. L. Chapter 17: Uplift and exposure of the Panamint metamorphic complex, California. In "Basin and Range Extensional Tectonics Near the Latitude of Las Vegas, Nevada". *Geological Society of America*, 345-362 (1990).

52. Izumi, N., Parker, G. & Yokokawa, M. Incisional cyclic steps of permanent form in mixed bedrock-alluvial rivers. *J. Geophys. Res. Earth Surf.* **122**(1), 130-152 (2017).

Acknowledgements

We acknowledge funding from: the National Natural Science Foundation of China 52109092 and U2340204 (LZ); the China Fundamental Research Funds for Central Universities 2023MS070 (LZ); and the W.H. Johnson Chair of the Department of Earth Science and Environmental Change, University of Illinois Urbana-Champaign (GP). We thank Aaron Yoshinobu and Suzanne Anderson for their helpful comments and advice, and Takuya Inoue for useful edits and comments.

Author information

School of Water Resources and Hydropower Engineering, North China Electric Power University, Beijing 102206, China.

Li Zhang, Shanghong Zhang

Department of Earth Science & Environmental Change and Department of Civil & Environmental Engineering, University of Illinois Urbana-Champaign, Urbana, IL 61801, USA.

Gary Parker

Department of Geosciences, Texas Tech University, Lubbock, TX 79409-1053, USA.

Jeffrey A. Nittrouer

Department of Hydraulic Engineering, Tsinghua University, Beijing 100084, China.

Xudong Fu, Guangqian Wang

Ethics declarations

Competing interests

The authors declare no competing interests.

Additional information

To be filled in if the paper is accepted for publication.

Table 1 | Values of parameters in the present study.

Parameter	Value	Notes
Q_w, m^3/s	29	Flood discharge
I_f	0.005	Flood intermittency fraction
D, mm	60	Grain size
B_c, m	20	Canyon bottom width
Cz	10	Chezy resistance coefficient
q_{af}, m^2/s	0.00134	Computed volume sediment transport rate/width during floods for prevailing conditions in Santa Rosa Wash
L, km	8	$L/2$ = initial length of canyon and $L/2$ = length of valley
β, km^{-1}	0.015	Abrasion coefficient for incision relation
λ	0.35	Porosity of alluvium
S_s	0.7	Canyon sidewall slope
S_{ci}	0.094	Initial canyon slope
S_{vi}	0.047	= $S_{ci}/2$, initial valley slope
S_p	0	Tableland slope

Figures

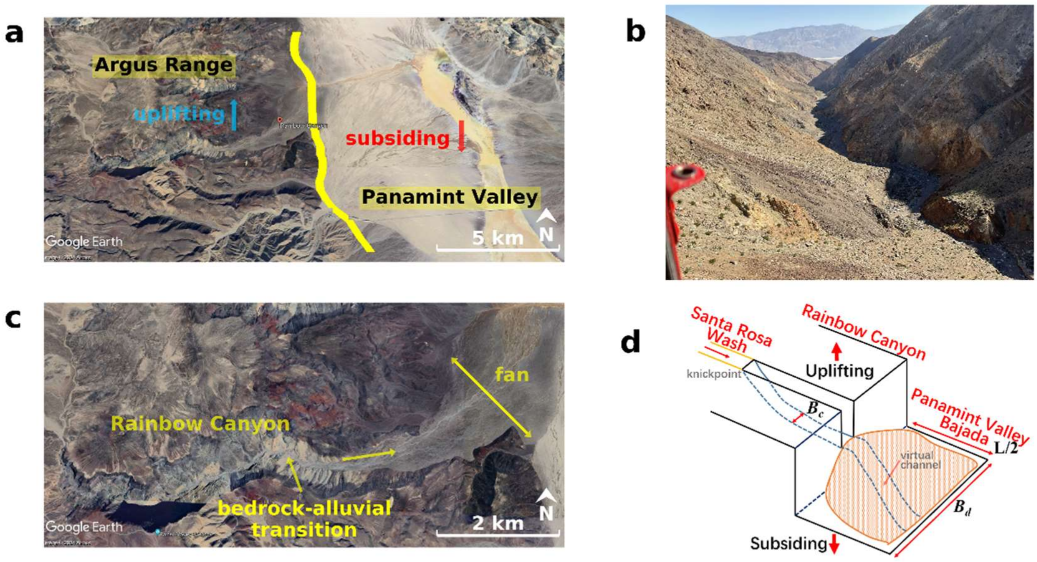

Fig. 1 | Setting for Rainbow Canyon and its corresponding fan in Panamint Valley. a, The Argus Range and Panamint Valley showing the fault line between the two. **b,** Helicopter view of Rainbow Canyon looking upstream on October 22, 2023. **c,** Rainbow Canyon and its corresponding fan, showing the position of the bedrock-alluvial transition upstream of the canyon mouth. **d,** Definition diagram for a simplified model of the canyon-fan system; symbols are defined in the text.

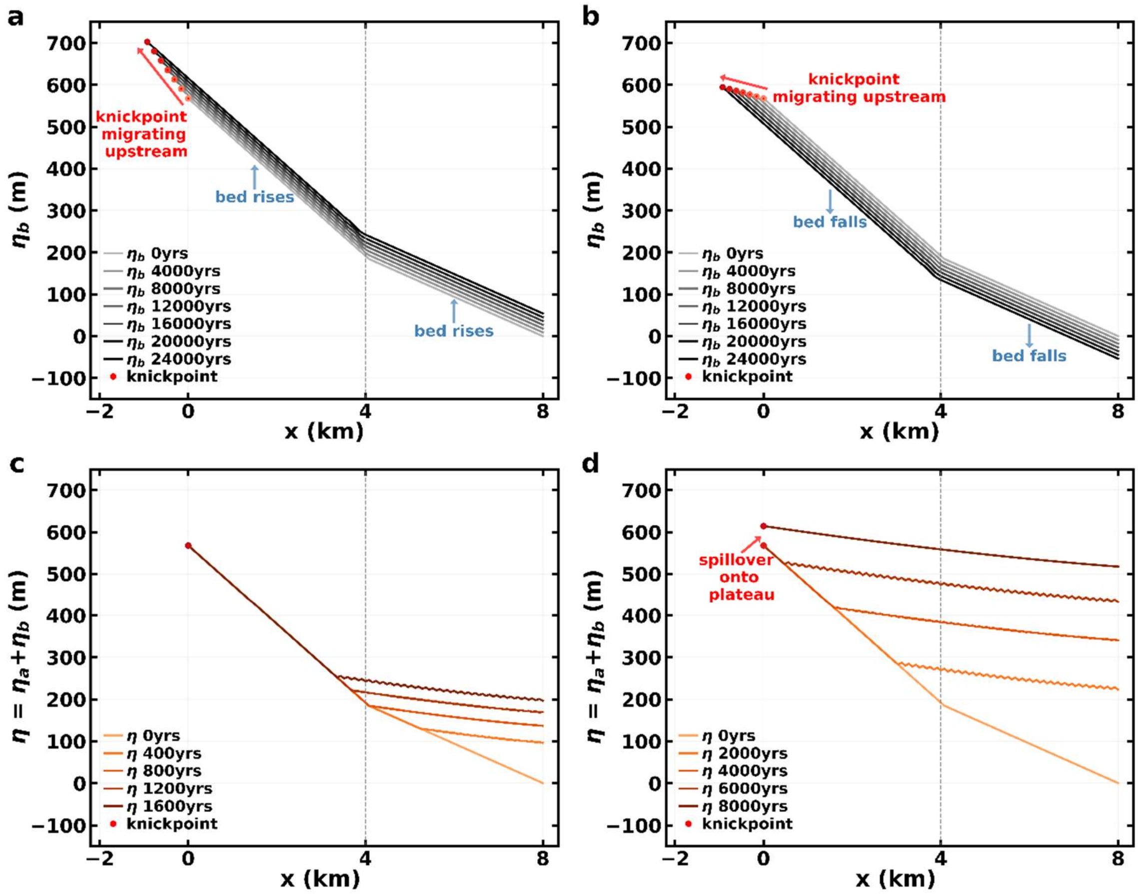

Fig. 2 | Behavior for pure incision and pure alluviation. a, Case of pure incision; no fan, slope $S_b = 0.094$ for upper reach and 0.047 for lower reach, $r = 1$, incision rate $E = 3$ mm/yr for upper reach and 2.74 mm/yr for lower reach (corresponding to the same sediment transport rate as upstream but half the slope), uplift rate $\upsilon = 5$ mm/year everywhere. **b,** Case of pure incision; no fan, all parameters identical to Fig. 2a except $\upsilon = 0.5$ mm/year everywhere. **c,** Case of pure alluviation; slope $S_b = 0.094$ for upper reach and 0.047 for lower reach, $r = 1$, $E = \upsilon = \sigma = 0$. **d,** Same as Case c, but calculation continued until sediment spills onto plateau.

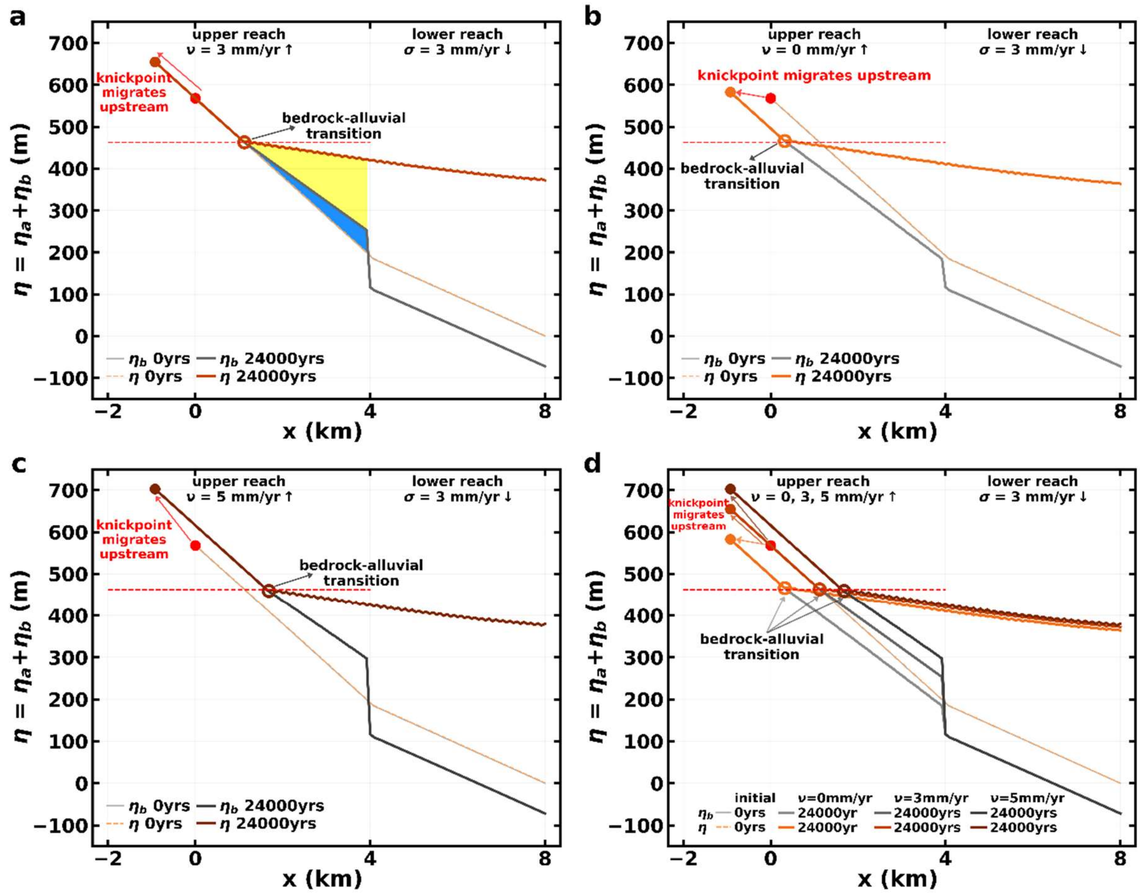

Fig. 3 | Behavior for canyon-fan interaction. In all cases r = 5, σ = 3 mm/year, E = 3 mm/year wherever bedrock is exposed and f_b = 0. **a,** υ = 3 mm/year. **b,** υ = 0 mm/year. **c,** υ = 5 mm/year. **d,** cases a), b) and c) plotted together. Note that the streamwise position of the bedrock-alluvial transition is displaced valleyward with increasing uplift rate, but the elevation of this transition remains constant. The results generalize for times other than 24,000 years.

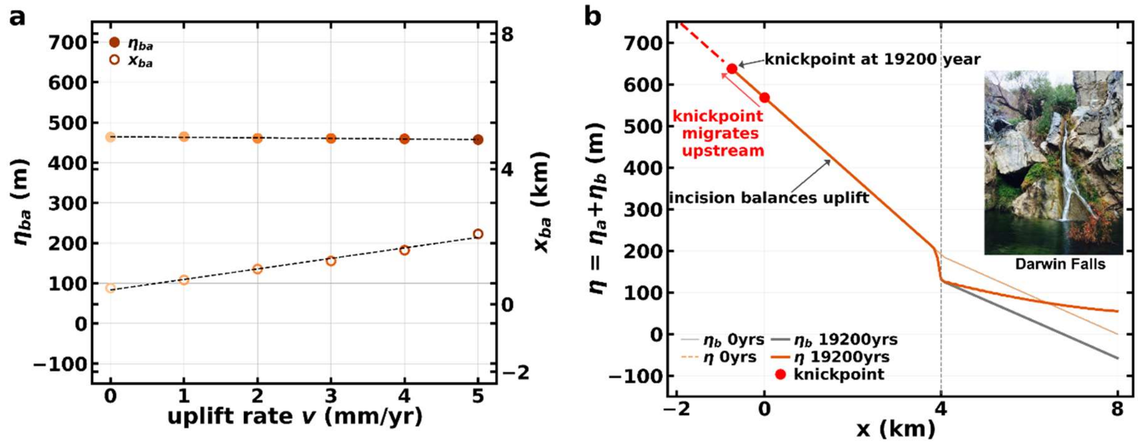

Fig. 4 | Communication between canyon and valley. a, Streamwise position x_{ba} and elevation η_{ba} of the bedrock-alluvial transition at 24,000 years for valley subsidence rate σ = 3 mm/year, bedrock incision rate E = 3 mm/year when exposed, uplift rate υ varies from 0 to 5 mm/year and ratio r of valley width to canyon width = 5. The variation of x_{ba} with υ is indicative of strong communication between canyon and valley. Elevation η_{ba}, however, remains independent of υ. **b,** Calculational results at 19,200 years for conditions that are the same as Fig. 3a ($\sigma = \upsilon = E$ = 3 mm/year) except that the valley is 8 times wider (r = 40). Under these conditions, the canyon and valley no longer communicate with each other. Instead, a vertical knickpoint, or waterfall forms. The example of Darwin Falls two canyons south of Rainbow Canyon is shown as an example in the inset.

Extended Figures

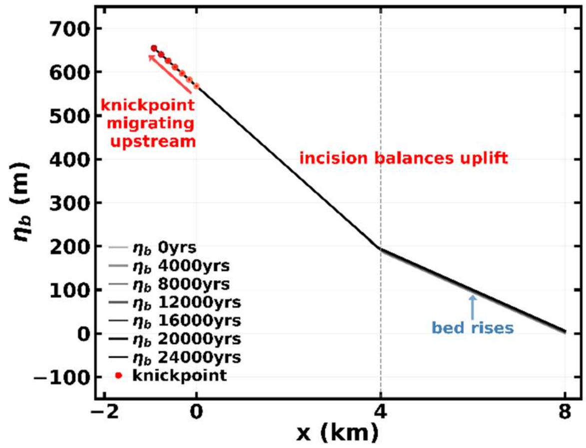

Extended Figure E1. This figure corresponds to Fig. 2 of the main text, but $E = \upsilon$ in the upper part of the domain. As a results, nothing happens there except upstream knickpoint migration. There is a slight rise in bed elevation in the lower part of the domain because bed slope is half that of the upper part with unchanged sediment transport, resulting in a lower incision rate.

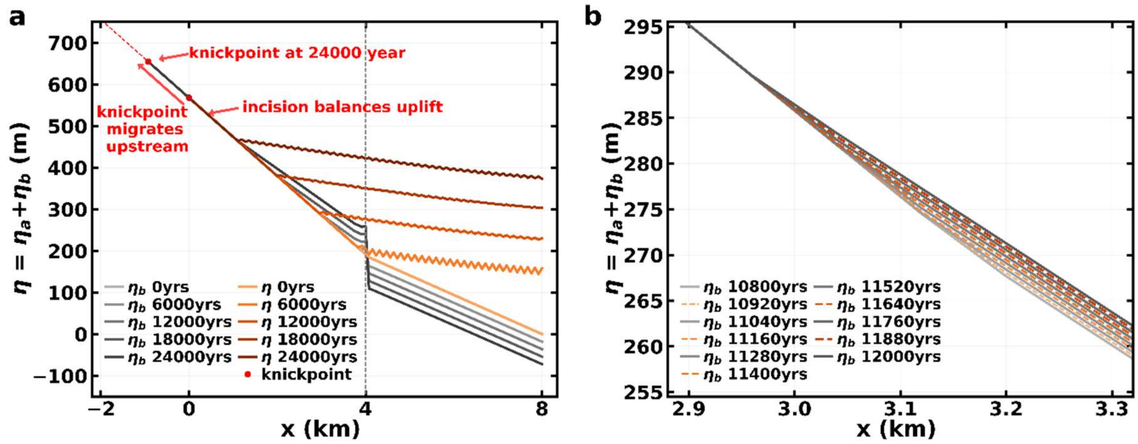

Extended Figure E2. The modeling conditions are the same as those of Fig. 3a, but with punctuated uplift of a sudden 0.72 m jump every 240 years. **a,** Bed elevation evolution within 24,000 years plotted to be comparable with Fig. 3a at sufficiently large spatial and temporal scales, the results are indistinguishable from the case of constant uplift of Fig. 3a. **b,** Expanded view of a short section upstream of the canyon-fan transition within 12,000 years, again demonstrating that the pulsed uplift is not recognizable at the time and space scales of the plot.

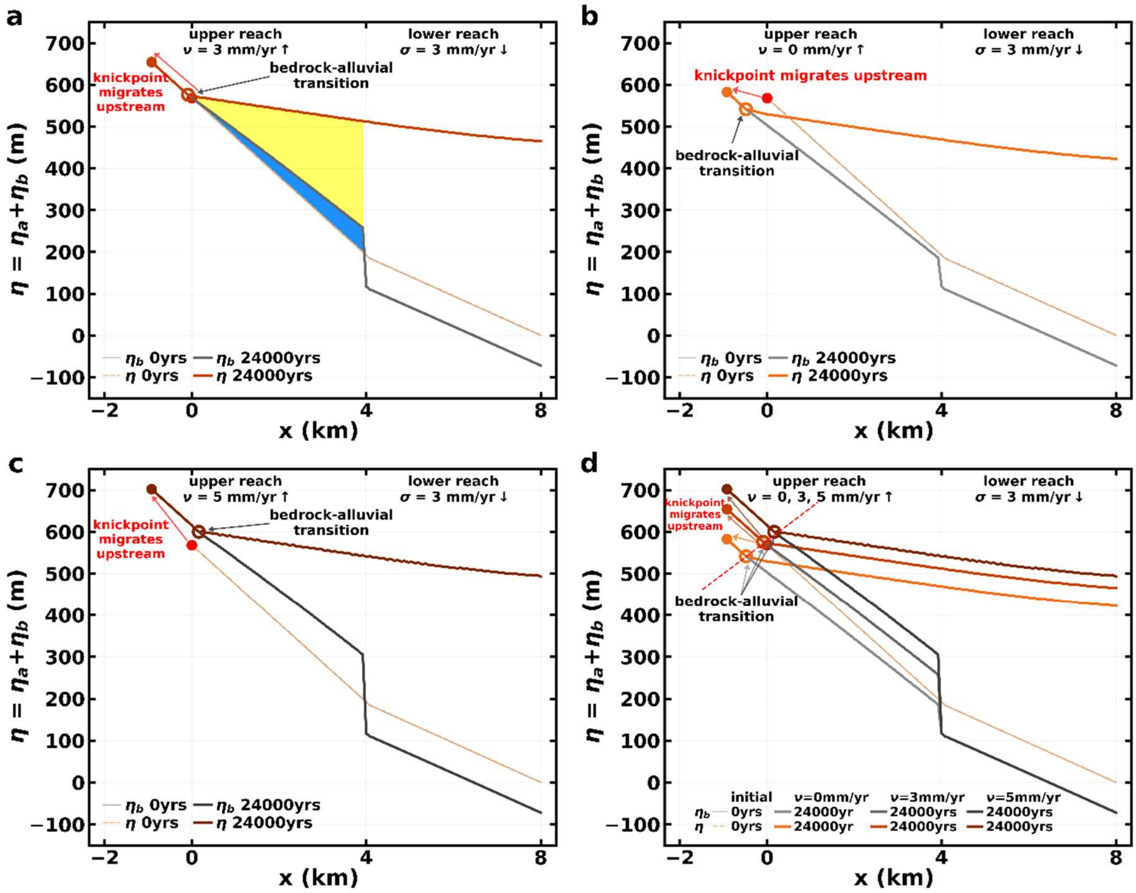

Extended Figure E3. Conditions are the same as Fig. 3 of the main text, except that sediment input from sidewall failure is allowed with $f_b = 0.25$. **a,** $\upsilon = 3$ mm/year. **b,** $\upsilon = 0$ mm/year. **c,** $\upsilon = 5$ mm/year. **d,** The three cases superimposed. The elevation η_{ba} of the bedrock-alluvial transition no longer remains invariant to uplift rate when sidewall input is included.

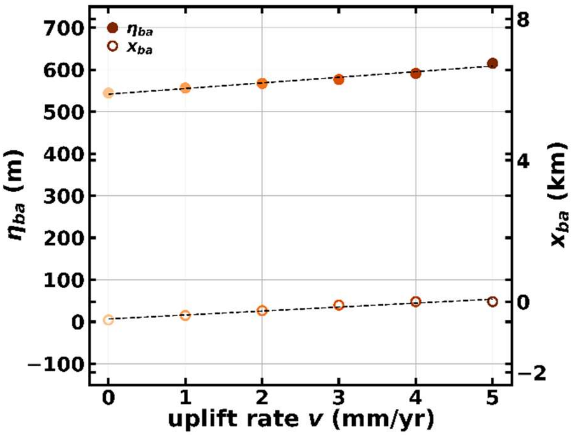

Extended Figure E4. The plot corresponds to Fig, 4a of the main text, except that sidewall sediment input is accounted for with $f_b = 0.25$. The streamwise position x_{ba} of the bedrock-alluvial transition moves downstream and the elevation η_{ba} increases with increasing uplift rate υ.

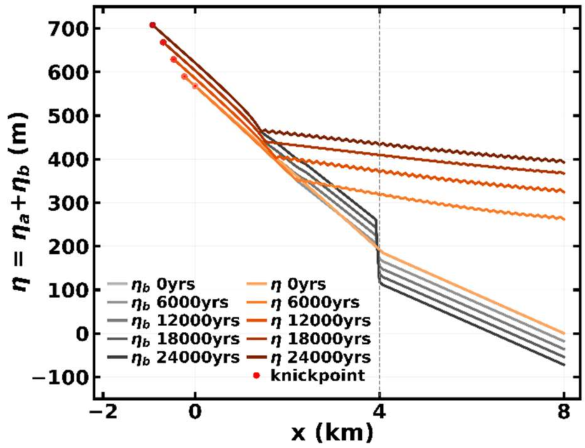

Extended Figure E5. This case is the same as that of Fig. 3a except that $f_b = 0.5$ and the sediment supply rate is cut by the factor 1/100 after 6000 years. The results illustrate the ability of the model to capture the effect of several interacting drivers, and shows the formation of an autogenic knickpoint within the canyon reach[8].